2024 4th International Conference on Emerging Frontiers in Electrical and Electronic Technologies (ICEFEET) | 979-8-3315-2861-4/24/$31.00 ©2024 IEEE | DOI: 10.1109/ICEFEET64463.2024.10866777

Voltage Accelerated Directional Overcurrent Relays for Microgrid Protection

Mahamad Nabab Alam
Dept. of Electrical Engineering
National Institute of Technology Warangal
Hanumakonda, India
mnalam@nitw.ac.in

***Abstract*—This paper proposes a voltage-accelerated directional overcurrent relay (VADOCR) based protection scheme for microgrids. The reduction in the fault current because of the domination of inverted-based renewable (IBR) power generation in microgrids has been taken care of by accelerating the operating time of relays through the fault voltage. This is achieved using a novel time-current-voltage characteristic of standard inverse definite minimum time relay. To compute the setting of the developed VADOCRs, the protection coordination problem has been formulated as an optimization problem and solved using a novel hybrid differential particle swarm optimization (DPSO) algorithm. To validate the proposed VADORCs and DPSO, the protection scheme for a standard 4-bus microgrid test system has been developed. The suitability and effectiveness of the obtained settings have been analysed. The proposed VADOCRs' overall performance is impressive and effective in protecting microgrids in the grid-connected and islanded modes of operation.**

***Index Terms*—Microgrids, Directional overcurrent relays, protection coordination, particle swarm optimization, inverted-based renewable sources.**

I. Introduction

AC microgrids are designed to enhance grid resilience, improve energy efficiency, and reduce dependency on fossil fuels. They operate in two modes: grid-connected or islanded. The microgrid synchronises with the main grid in the grid-connected mode, allowing energy exchange. When operating in islanded mode, the microgrid functions autonomously, providing continuous energy to the local area even if the main grid experiences an outage [1]. Solar power generation is locally connected to the grid wherever it is available such as rooftop solar power plants [2].

Despite these benefits, AC microgrids introduce various technical challenges, particularly regarding protection mechanisms. Electrical protection is crucial for safeguarding equipment, ensuring the safety of personnel, and maintaining the stability and reliability of the power system. Conventional protection systems designed for large, centralized grids are often inadequate for the unique characteristics of microgrids. Several specific protection challenges arise within AC microgrids [3]. Following are some of the key challenges:

1) Bidirectional Power Flow
2) Dynamic Operating Modes
3) Low Short-Circuit Currents
4) Intermittent Renewable Energy Sources
5) Coordination of Protection Devices

In traditional power grids, electricity flows unidirectionally from utilities to consumers. In contrast, AC microgrids allow for bidirectional power flow, especially those using renewable energy sources like solar and wind. This complexity complicates fault detection and location, as conventional protection systems are not equipped to handle changing power flow directions, leading to delays in response and increased system risks.

Additionally, switching between grid-connected and islanded modes poses challenges. In islanded mode, the microgrid loses stabilization from the larger grid, resulting in potential voltage and frequency fluctuations that traditional protection schemes may not handle effectively. Protection devices must adapt quickly and reliably to these changing conditions, a complex task in a decentralized environment.

Microgrids that rely on inverter-based resources, such as solar PV and battery systems, produce lower short-circuit currents than traditional power plants. This reduction can hinder overcurrent protection devices, which depend on higher fault currents for effective operation. Consequently, microgrids require more sensitive and advanced protection strategies to manage faults under low short-circuit conditions.

The integration of intermittent renewable energy sources further complicates protection design. Fluctuations in energy generation can lead to instability in voltage and frequency, affecting the performance of protective devices and making fault detection more challenging as system behaviour changes with solar or wind power availability.

In AC microgrids, coordinating multiple protection devices is essential for selective fault isolation. However, achieving this coordination amidst varying fault currents, bidirectional flows, and dynamic operating modes is difficult. Miscoordination can result in unnecessary disconnections of healthy grid parts or delays in fault isolation, undermining the overall reliability of the system [4].

The coordination of DOCRs has been extensively researched in the literature [5]. Optimization-based techniques are particularly favoured for addressing the protection coordination challenge by determining optimal relay settings. This issue is commonly modelled as an optimization problem, with various optimization algorithms applied to find solutions. Nonlinear programming (NLP) formulations are frequently used, and analytical and heuristic approaches have been explored in previous work. Analytical methods such as the interior-point method [6] and the sequential quadratic programming [7] have been well-studied in this context. On the heuristic side, algorithms such as particle swarm optimization (PSO) and differential evolution (DE) [8] are among the most widely utilized techniques for solving DOCR protection coordination problems. For the protection of AC microgrids, several different types of protection schemes have been studied in the literature [1], [3], [9]. However, proper protection coordination for microgrids is still a challenging task because the functionality of the relays depends on fault current, which is relatively low in the case of an islanded mode of operation. Most of the relay fails to perform well under lower fault current cases. This paper aims to provide adequate protection under the islanded and grid-connected operation of microgrids.

This paper presents a voltage-accelerated directional overcurrent relay (VADOCR) protection scheme for microgrids. It addresses the challenge of reduced fault current caused by the prevalence of inverter-based renewable (IBR) energy in microgrids by speeding up relay operation times based on fault voltage levels. This is accomplished through a novel time-current-voltage characteristic for standard inverse definite minimum time relays. To determine the optimal settings for the VADOCRs, the protection coordination challenge is formulated as an optimization problem, which is solved using a new hybrid differential particle swarm optimization (DPSO) algorithm. The effectiveness of the proposed VADOCRs and DPSO method is demonstrated through a protection scheme developed for a standard 4-bus microgrid test system.

II. Problem Statement

A. Protection Coordination Issues

The protection coordination between primary-backup relay pairs (OCRs/DOCRs) is evaluated based on the coordination time interval (CTI), defined as:

$$CTI = t_{ob} - t_{op} \tag{1}$$

where the relay operating time is derived from its time-current characteristic (TCC). An IDMT-type of OCR with a standard inverse TCC is typically used in power distribution networks. The operating time (t_{op}) of the relay is a function of its time multiplier setting (TMS) and pickup current setting or plug setting (PS) for a given fault current (I_f). The standard TCC is given by the following:

$$t_{op} = \frac{0.14 \times TMS}{\left(\frac{I_f}{PS}\right)^{0.02} - 1} \tag{2}$$

Here, *TMS* and *PS* are the relay settings, and the operating times of the primary (t_{op}) and backup relays (t_{ob}) can be calculated using this equation. The ratio I_f/PS is the plug setting multiplier (PSM).

The CTI value determines coordination. Coordination *holds* if CTI exceeds the minimum coordination time (MCT), and is *lost* otherwise. The conditions for coordination are:

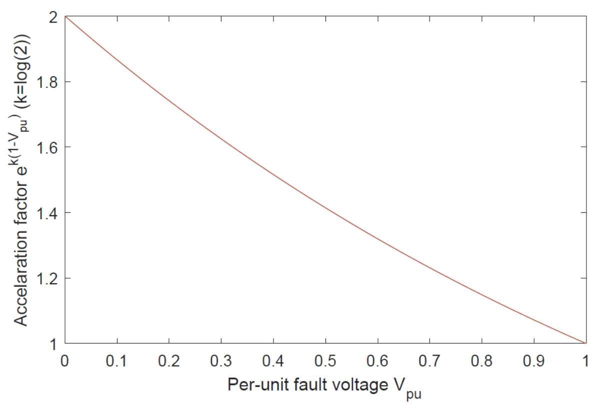

Fig. 1. Voltage dependent acceleration factor.

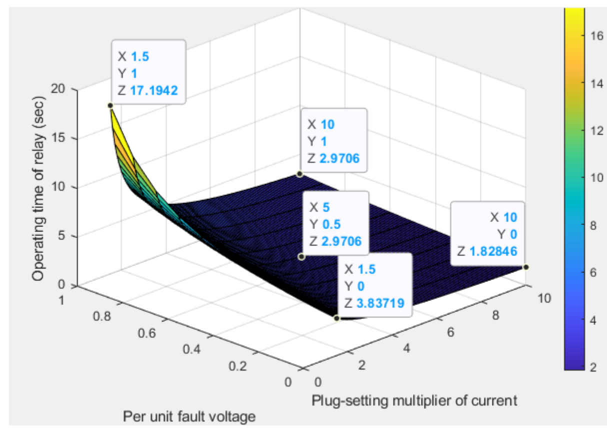

Fig. 2. Time-current-voltage characteristic of the proposed VADOCR.

- CTI $\geq$ MCT: coordination *holds*
- CTI $<$ MCT: coordination *lost*

The MCT typically ranges between 0.2–0.3 seconds, ensuring the primary relay has sufficient time to operate before the backup relay acts.

B. Proposed Voltage Accelerated DOCR Characteristic

The novel time-current-voltage characteristic of standard inverse definite minimum time relay is mathematically expressed as follows:

$$t_{op} = \frac{0.14 \times TMS}{\left(\frac{I_f \times e^{k(1-V_{pu})}}{PS}\right)^{0.02} - 1} \tag{3}$$

where V_{pu} is the value of per-unit fault voltage at the relay location, k is the voltage deviation coefficient, and $e^{k(1-V_{pu})}$ is the voltage acceleration factor which enhances the operating time of the relay at the lower fault current. The value of k varies from 0 to 0.6931 to accelerate the PSM by up to 2 times using voltage drop because of the fault. Figs. 1 and 2 show the proposed time-current-voltage characteristic of the proposed VADOCR.

A few key points are indicated in Fig. 2 to show the impact of the voltage acceleration factor, which causes a reduction in the operating time of the relay even if the PSM is the same.

C. Problem Formulation

The protection coordination problem of DOCRs is formulated as an optimization problem. The objective is to minimize the weighted sum of the operating times of all DOCRs, subject to coordination constraints, ensuring a minimum time gap between the operating times of primary-backup relay pairs and limits on related parameters.

Mathematically, the problem is defined as:

$$OF = \min\left(\sum_{k=1}^{m} t_{op,k}^2 + \sum_{k=1}^{m} t_{ob,k}^2 + \sum_{k=1}^{m}(t_{ob,k} - t_{op,k})^2\right) \tag{4}$$

Subject to:

$$t_{ob,j} - t_{op,i} \geq MCT \tag{5}$$

$$TMS_{min} \leq TMS_k \leq TMS_{max} \tag{6}$$

$$PS_{min} \leq PS_k \leq PS_{max} \tag{7}$$

$$t_{min} \leq t_{op,k} \leq t_{max} \tag{8}$$

In this formulation, $t_{op,k}$ is the operating time of relay R_k; $t_{op,i}$ and $t_{ob,j}$ are the operating times of primary relay R_i and backup relay R_j, respectively; TMS_{min} and TMS_{max} are the limits on TMS; PS_{min} and PS_{max} are the limits on the PS t_{min} and t_{max} are the minimum and maximum operating times of relay R_k; and m is the total number of relay pairs in the system. The total number of relays is assumed to be n with a m number of relay pairs. A fitness function is defined for this problem as $F = OF + PenaltyFactor \times ConstraintViolation$ which is used in the optimization.

Some primary backup relay pairs have backup relays experiencing much lower fault currents than the primary relay, and these pairs always satisfy the MCT requirement. To reduce the computational burden, such pairs should be excluded when solving the protection coordination problem. These relay pairs meet the following conditions:

$$I_{fback} < \max(2 \times I_{Lmax}, I_{fmin}) \tag{9}$$

where I_{fback} is the fault current through the backup relay, I_{Lmax} is the maximum load current, and I_{fmin} is the minimum fault current encountered by the backup relay.

The CT ratio is typically selected based on the maximum load current. The primary rating is determined by the maximum load current and the highest short-circuit current it may experience to prevent CT saturation. The primary rating of the CT for relay R_i is chosen as the next higher standard value of CTP_i, calculated as:

$$CTP_i = \max\left(I_{Lmax,i}, \frac{I_{fmax,i}}{20}\right) \tag{10}$$

The maximum load current is $I_{Lmax,i}$, while $I_{fmax,i}$ represents the maximum three-phase fault current passing through relay R_i. The current transformer (CT) ratio for each relay R_i is $CTP_i : 1$. All CTs have been considered protection class 5P20, ensuring that up to 20 times rated current CT will not saturate.

To address the formulated problem, the following constraints have been applied:

- The TMS is constrained within the range $[0.1, 1.1]$
- The PS is constrained within the range $[0.5, 2.0]$
- $k = 0.6931$ has been considered for VADOCRs to give an acceleration factor of 2 (maximum)
- The primary relays operation is restricted to $[0.1, 2]$ sec
- The MCT requirement is set to 0.2 sec

III. Proposed Differential Particle Swarm Optimization Approach

The formulated problem has been solved using the differential particle swarm optimization (DPSO) algorithm which is a hybrid algorithm comprising differential evolution (DE) and particle swarm optimization (PSO) algorithms.

The DPSO algorithm updates particle positions using two equations based on personal best (Pbest), global best (Gbest), current velocity, and differential position. The experience is influenced by three factors, c_1, c_2 and c_3, along with three uniformly distributed random numbers r_1, r_2, and r_3 in $[0, 1]$. The current velocity is scaled by an inertia weight w whose value varies between $[0.4, 0.9]$.

The initial population (swarm) consists of N particles, each with D dimensions, and is represented as $\mathbf{X} = [\mathbf{X}_1, \mathbf{X}_2, \ldots, \mathbf{X}_N]^T$. Each particle $\mathbf{X}_i$ $(i = 1, 2, \ldots, N)$ is defined by a vector $\mathbf{X}_i = [X_{i1}, X_{i2}, \ldots, X_{iD}]$, where i denotes the particle index and j refers to the dimension. The velocity of each particle is similarly expressed as $\mathbf{V} = [\mathbf{V}_1, \mathbf{V}_2, \ldots, \mathbf{V}_N]^T$, with $\mathbf{V}_i = [V_{i1}, V_{i2}, \ldots, V_{iD}]$. The indices i range from 1 to N, and j from 1 to D. The DPSO algorithm updates particles using the following equations:

$$\begin{aligned} V_{ij}^{k+1} = wV_{ij}^k + c_1 r_1 (P_{ij}^k - X_{ij}^k) \\ + c_2 r_2 (G_j^k - X_{ij}^k) + c_3 r_3 (X_{yj}^k - X_{zj}^k) \end{aligned} \tag{11}$$

$$X_{ij}^{k+1} = X_{ij}^k + V_{ij}^{k+1} \tag{12}$$

Here, P_{ij}^k is the personal best position of the i-th particle, and G_j^k is the global best position up to iteration k. In eq. (11), c_3 is the scaling factor and r_3 is a randomly generated random number in 0 and 1 whereas y and z represent two distinct randomly selected particles corresponding to target particle i. In this equation y and z varies from 1 to N but $y \neq z \neq i$. This term brings diversity in the velocity vector, which causes each particle to escape from the local minima. The last component of eq. (11) is inspired by DE, whereas the first three terms are associated with PSO. Hence, the name DPSO is given to this hybrid algorithm.

The protection coordination problem of DOCRs, as outlined in the previous section, presents significant complexity. To address this, the proposed DPSO algorithm has been employed within the MATLAB environment to determine the optimal settings for the relays.

Two key variables - TMS and PS, have been used in this formulation. These variables represent the particles in the DPSO algorithm. The configuration of relay settings, or the "particle," is defined as follows:

Particle = | **TMS** | **PS** |

where **TMS** = $[TMS_1, TMS_2, ..., TMS_n]$ and **PS** = $[PS_1, PS_2, ..., PS_n]$. The steps of the proposed DPSO are given in **Algorithm 1**.

Algorithm 1 Proposed DPSO Algorithm

1: Read various datasets required for the study
2: Fix DPSO parameters N, D, c_1, c_2, c_3, and $Maxite$
3: Randomly initialize position **X** of the population
4: Randomly initialize velocity **V** of the population
5: Start iteration count $k = 1$
6: Evaluate fitness $F_i^k = f(\mathbf{X}_i^k), \forall i$ and identify the best particle b among the population
7: Identify personal and global bests $P_{ij}^k = X_{ij}^k, \forall ij$ and $\mathbf{G}^k = \mathbf{X}_b^k$
8: Update velocity using eq. (11) and position using eq. (12) for the entire population
9: Evaluate updated fitness as $F_i^{k+1} = f(\mathbf{X}_i^{k+1}), \forall i$ and identify new best particle b_k
10: Update Pbest of the population in the next step
11: **if** $F_i^{k+1} \leq F_i^k$ **then**
12: $\quad P_{ij}^{k+1} = X_{ij}^{k+1}, \forall j$
13: **else** $P_{ij}^{k+1} = P_{ij}^k, \forall ij$
14: **end if**
15: Update Gbest of the population in the next step
16: **if** $F_{b1}^{k+1} \leq F_b^k$ **then**
17: $\quad \mathbf{G}^{k+1} = \mathbf{X}_{b_kj}^{k+1}, \forall j$ and set $b = b_k$
18: **else** $\mathbf{G}^{k+1} = \mathbf{G}^k$
19: **end if**
20: Check stopping criteria in the next step
21: **if** $k \leq Maxite$ **then**
22: $\quad Goto$ step 8
23: **else**
24: $\quad Goto$ step 26
25: **end if**
26: Print $\mathbf{G}^k$ and get TMS and PS of all relays

In this study, the following parameters have been considered for the developed DPSO algorithm: population size 100, maximum iteration limit 40000, stall iteration limit 400, $c_1 = c_2 = 2.025$, $c_3 = 0.0001$, $w = 0.729$ and initial velocity as 20% of the position of the population, i.e., $\mathbf{V} = 0.2\mathbf{X}$. The penalty factor for constraint violation is considered as 10000. These values have been fixed after repeated runs with a wide range of these values.

IV. Simulation Results and Discussion

The proposed protection coordination approach is validated on a 4-bus microgrid test system. The single-line diagram (SLD) of this system is shown in Fig. 3. Three distributed generators (DGs) are connected at buses B2, B3, and B4. DG1 is a synchronous generator, while the others are solar photovoltaic DGs. The necessary parameters for the network are indicated in the SLD. Eight sets of DOCRs are used to protect the lines in the system. Each DG has a relay at its terminal to protect against excessive fault current when faults occur on the DG side.

Each set of DOCRs includes three-phase relays and an earth fault relay to protect against all ten types of faults. These relays, denoted as $R1, R2, \ldots, R8$ in Fig. 3, are configured with proper protection coordination to ensure the primary and backup relays operate according to the coordination criteria. Phase relay settings consider protection coordination, while earth fault relay settings depend on the maximum allowable unbalance at their location. The relays are directional and set to protect the lines from a fault on that line.

The system is modelled in SIMULINK to calculate load currents, fault currents and fault voltages. The voltage and current measurements have been taken from each line's terminals, i.e., at the bus under any fault location. In actual systems, measurements are only available through current and voltage transformers at the line ends. Also, the per-unit voltage considered corresponds to the phase-to-ground voltage. The base values of power and voltage are mentioned in the SLD. Table I provides the load and fault currents for the eight DOCRs, while Table II lists the fault currents and per-unit voltages required for protection coordination of the ten primary backup relay pairs under different types of network operating conditions and fault locations. For simplicity, only three-phase faults were applied to collect the necessary data.

Eight relays are installed (two at each line at their ends), resulting in 10 primary backup relay pairs. Fault simulations are performed at the near-end, far-end, and mid-point of the lines. Considering both grid-connected and islanded modes of operation, there are 45 primary backup relay pairs in total, as shown in Table II. It is to be noted that the number of relay pairs is different in grid-connected and islanded modes because the fault current flow patterns are different, and the listed primary backup relay currents are in the forward direction for which they are supposed to operate for a fault. Except for near-end faults in grid-connected mode, the other types of faults, a few pairs have seen current in the reverse direction by their primary relays, and hence, they have been ignored and not listed in this table.

TABLE I
Various Load and Fault Currents Through Each Relay

Relays	I_{Lmax} (A)	V_{Lmax} (pu)	I_{fmax} (A)	V_{fmax} (pu)	I_{fmin} (A)	V_{fmin} (pu)
1	617	0.941	5475	0.001	2220	0.602
2	–	1.000	4106	0.001	2721	0.313
3	228	0.950	7099	0.001	769	0.209
4	–	1.000	2040	0.001	230	0.339
5	246	0.950	7031	0.001	703	0.214
6	–	1.000	2159	0.001	272	0.344
7	38	0.897	3343	0.001	519	0.119
8	15	0.904	3525	0.001	68	0.052

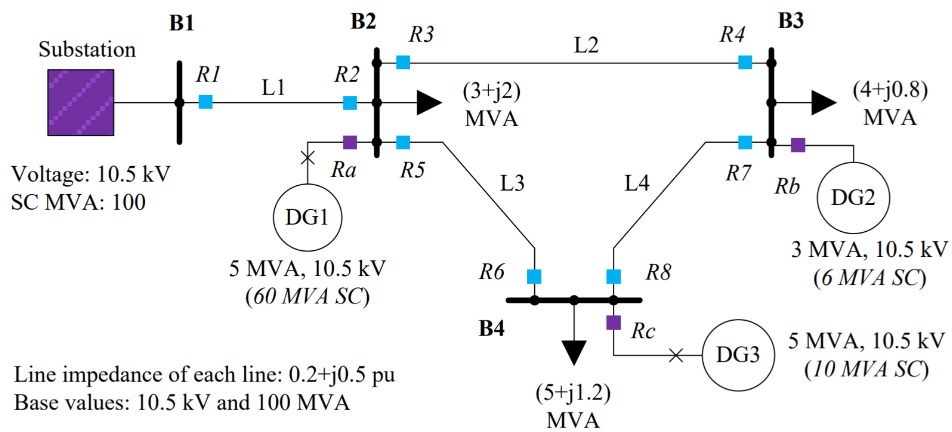

Fig. 3. 4-bus microgrid test system.

TABLE II
PRIMARY BACKUP RELAY PAIRS AND CORRESPONDING FAULT CURRENTS AND FAULT VOLTAGES

Microgrid mode	Faults location	Relay pairs	Primary Relay	Backup Relay	I_{fpr} (A)	V_{fpr} (pu)	I_{fbr} (A)	V_{fbr} (pu)
Grid-connected	L1-near	1	2	4	4106	0.001	377	0.044
	L1-near	2	2	6	4106	0.001	445	0.052
	L2-near	3	3	1	7099	0.001	3377	0.389
	L2-near	4	3	6	7099	0.001	445	0.052
	L2-near	5	4	8	2040	0.001	1713	0.197
	L3-near	6	5	1	7031	0.001	3377	0.389
	L3-near	7	5	4	7031	0.001	377	0.044
	L3-near	8	6	7	2159	0.001	1613	0.186
	L4-near	9	7	3	3343	0.001	3016	0.347
	L4-near	10	8	5	3525	0.001	2980	0.343
Grid-connected	L1-far	11	2	4	2721	0.313	230	0.339
	L1-far	12	2	6	2721	0.313	273	0.344
	L2-far	13	3	1	3016	0.347	2220	0.602
	L2-far	14	4	8	377	0.044	68	0.052
	L3-far	15	5	1	2980	0.343	2233	0.600
	L4-far	16	7	3	1613	0.186	1367	0.343
	L4-far	17	8	5	1713	0.197	1304	0.347
Grid-connected	L1-mid	18	2	4	3272	0.189	287	0.222
	L1-mid	19	2	6	3272	0.189	340	0.228
	L2-mid	20	3	1	4368	0.253	2538	0.544
	L2-mid	21	4	8	1261	0.074	986	0.187
	L3-mid	22	5	1	4350	0.251	2543	0.543
	L3-mid	23	6	7	1364	0.079	872	0.179
	L4-mid	24	7	3	2358	0.136	2091	0.376
	L4-mid	25	8	5	2478	0.143	2031	0.376
Islanded	L1-near	26	2	4	4106	0.001	377	0.044
	L1-near	27	2	6	4106	0.001	445	0.051
	L2-near	28	3	6	3730	0.001	445	0.051
	L2-near	29	4	8	1486	0.001	1158	0.133
	L3-near	30	5	4	3862	0.001	377	0.044
	L3-near	31	6	7	1591	0.001	1044	0.120
	L4-near	32	7	3	2188	0.001	1860	0.214
	L4-near	33	8	5	2360	0.001	1812	0.207
Islanded	L1-far	34	2	4	2722	0.313	230	0.339
	L1-far	35	2	6	2722	0.313	272	0.344
	L2-far	36	4	8	377	0.044	68	0.051
	L4-far	37	7	3	1044	0.120	769	0.209
	L4-far	38	8	5	1158	0.133	703	0.214
Islanded	L1-mid	39	2	4	3273	0.188	287	0.221
	L1-mid	40	2	6	3273	0.188	340	0.222
	L2-mid	41	4	8	949	0.055	642	0.128
	L3-mid	42	5	4	2550	0.147	243	0.119
	L3-mid	43	6	7	1026	0.059	519	0.119
	L4-mid	44	7	3	1564	0.090	1275	0.237
	L4-mid	45	8	5	1691	0.097	1211	0.097

The CT ratio for each relay is calculated using the approach discussed earlier in this section and is given in Table III.

TABLE III
CT RATIOS AND BOUNDS ON PS VALUES OF EACH RELAY

Relays	CTR	Relays	CTR
1	600:1	5	250:1
2	200:1	6	100:1
3	250:1	7	150:1
4	100:1	8	50:1

The optimum setting of the relays has been computed using DPSO for three cases. The first one is under grid-connected mode of microgrid operation. The second one is under the islanded mode of microgrid operation. However, the third case combines grid-connected and islanded microgrid operation modes.

The optimum settings of the relays obtained considering the proposed formulation and DPSO corresponding to all three scenarios are in Table IV. Similarly, the sum of operating times of all primary relays, backup relays and their CTI values are given in Table V. Also, the CTI for each primary backup relay pair has been plotted in Figs. 4, 5 and 6 for all three case. It is to be noted that for grid-connected mode, relay pairs are from 1-25 as listed in Table II. Similarly, relay pairs are from 26 to 45 serial numbers for the islanded mode case, as listed in Table II.

TABLE IV
OPTIMUM SETTINGS VADOCRS USING DPSO ALGORITHM FOR 4-BUS MICROGRID TEST SYSTEM

Relays	Grid-Connected Mode		Islanded Mode		Both Modes	
	TMS	PS	TMS	PS	TMS	PS
1	0.2960	0.6684	0.4447	1.8967	0.3285	0.6125
2	0.2703	0.7807	0.3367	0.9878	0.2791	1.8960
3	0.2797	1.7420	0.2720	1.6292	0.3079	1.5495
4	0.2518	1.0657	0.2702	1.4329	0.2327	1.9128
5	0.2863	1.7674	0.4373	0.5000	0.4295	0.5058
6	0.2555	1.1374	0.2289	1.8288	0.3095	1.0734
7	0.3304	0.8082	0.3641	0.5000	0.2948	1.7159
8	0.4627	0.5684	0.5223	0.5000	0.4504	0.8137
$\sum t_{op,main}$	3.5420 sec		4.3557 sec		3.9483 sec	

From Table IV, it is observed that the sum of operating times of all the 8 VADOCRs are 3.5420, 4.3557 and 3.9483

TABLE V
SUM OF OPERATING TIMES OF RELAYS UNDER DIFFERENT CASES

Microgrid operation	Relay pairs	$\sum t_{op}$ (sec)	$\sum t_{ob}$ (sec)	$\sum CTI$ (sec)	$\sum(t_{op} + t_{ob} + CTI)$ (sec)
Grid-connected	25	12.5174	19.9555	7.4381	39.9110
Islanded	20	11.6939	18.3742	6.6805	36.7486
Both modes	45	26.2894	41.7134	15.4237	83.4265

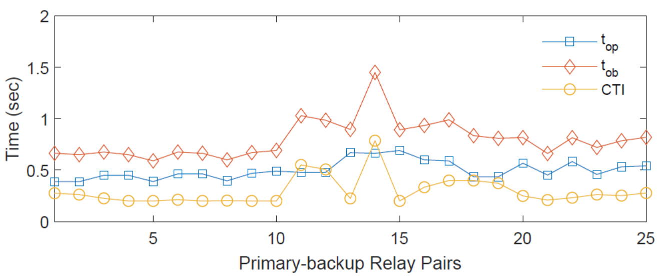

Fig. 4. CTI of relays pairs for grid-connected mode.

seconds for grid-connected, islanded and both grid-connected and islanded modes of microgrid, respectively. These operating times have been calculated considering the maximum values of fault calculation details of Table I. From Table V, it is quite clear that the sum of the operating times of relays under grid-connected and islanded modes is less than that of both grid-connected and islanded microgrid operation modes. This is because the settings calculated under grid-connected will work well for grid-connected mode only, not for the islanded mode of microgrid operation and vice-versa. However, the VADORCs setting calculated under both considerations can provide proper protection coordination under grid-connected and islanded modes of microgrid operation. Therefore, although the operating times of relays are higher in both cases, the settings are appropriate to provide full protection of microgrids.

From Figs. 4, 5, and 6, it is observed that all three cases of the system maintain the MCT requirement of 0.2 seconds. Hence, it is evident that the proposed VADORCs and DPSO-based protection coordination scheme perform well and are suitable for properly protecting microgrids under both grid-connected and islanded modes of operation.

V. CONCLUSION

This paper introduces a voltage-accelerated directional overcurrent relay (VADOCR) protection scheme tailored for microgrids, addressing the challenge of reduced fault currents due to the increased presence of inverter-based renewable (IBR) power generation. The proposed scheme accelerates the relay's response by incorporating fault voltage into the relay's operating time. A novel time-current-voltage characteristic of the inverse definite minimum time relay has enhanced performance. The protection coordination problem was formulated as an optimization task and solved using a hybrid differential particle swarm optimization (DPSO) algorithm. The effectiveness of the proposed VADOCRs was validated using a standard 4-bus microgrid test system, and the results demonstrate that the scheme effectively safeguards microgrids in both grid-connected and islanded modes. The overall performance of VADOCRs shows promise in providing robust and reliable protection for modern microgrid systems.

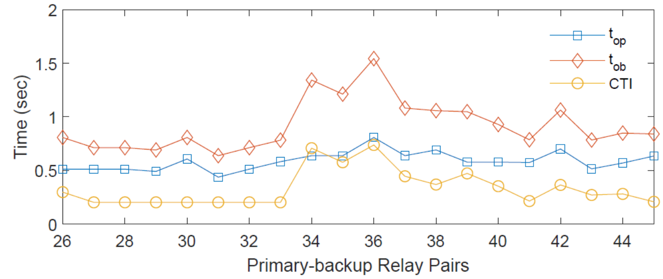

Fig. 5. CTI of relays pairs for islanded mode.

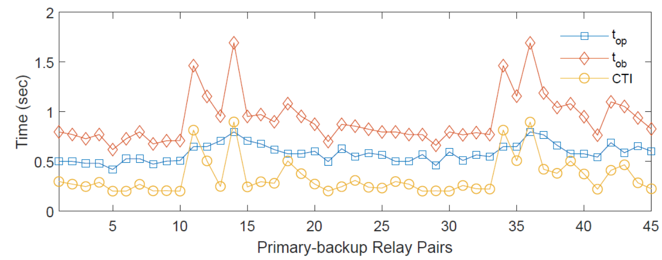

Fig. 6. CTI of relays pairs for grid-connected and islanded modes.

The future scope of this work will focus on providing the optimum settings considering mixed-characteristic curves of voltage-accelerated directional overcurrent relays for microgrids and networked microgrids.

REFERENCES

[1] A. A. Memon and K. Kauhaniemi, "A critical review of ac microgrid protection issues and available solutions," *Electric Power Systems Research*, vol. 129, pp. 23–31, 2015.

[2] S. Saha and R. Mandal, "RCPI controller-based multilevel multistring grid following inverter for large rooftop PV power plant application," *Electr Eng*, 2024.

[3] A. Hooshyar and R. Iravani, "Microgrid protection," *Proceedings of the IEEE*, vol. 105, no. 7, pp. 1332–1353, 2017.

[4] M. N. Alam, "Overcurrent protection of AC microgrids using mixed characteristic curves of relays," *Computers & Electrical Engineering*, vol. 74, pp. 74 – 88, 2019.

[5] D. S. Alkaran, M. R. Vatani, M. J. Sanjari, G. B. Gharehpetian, and A. H. Yatim, "Overcurrent relays coordination in interconnected networks using accurate analytical method and based on determination of fault critical point," *IEEE Transactions on Power Delivery*, vol. 30, no. 2, pp. 870–877, April 2015.

[6] M. N. Alam, B. Das, and V. Pant, "An interior point method based protection coordination scheme for directional overcurrent relays in meshed networks," *International Journal of Electrical Power Energy Systems*, vol. 81, pp. 153–164, 2016.

[7] K. A. Saleh, M. S. El Moursi, and H. H. Zeineldin, "A new protection scheme considering fault ride through requirements for transmission level interconnected wind parks," *IEEE Transactions on Industrial Informatics*, vol. 11, no. 6, pp. 1324–1333, 2015.

[8] M. N. Alam, B. Das, and V. Pant, "A comparative study of metaheuristic optimization approaches for directional overcurrent relays coordination," *Electric Power Systems Research*, vol. 128, pp. 39–52, 2015.

[9] A. Hooshyar and R. Iravani, "A new directional element for microgrid protection," *IEEE Transactions on Smart Grid*, vol. 9, no. 6, pp. 6862–6876, 2018.